Realizing Topological Superconductivity in Tunable Bose-Fermi Mixtures with Transition Metal Dichalcogenide Heterostructures

Caterina Zerba,[1,2] Clemens Kuhlenkamp,[1,2,3] Ataç Imamoğlu,[3] and Michael Knap[1,2]
[1]Technical University of Munich, TUM School of Natural Sciences, Physics Department, 85748 Garching, Germany
[2]Munich Center for Quantum Science and Technology (MCQST), Schellingstrasse 4, 80799 München, Germany
[3]Institute for Quantum Electronics, ETH Zürich, CH-8093 Zürich, Switzerland

(Received 16 October 2023; accepted 21 June 2024; published 30 July 2024)

Heterostructures of two-dimensional transition metal dichalcogenides are emerging as a promising platform for investigating exotic correlated states of matter. Here, we propose to engineer Bose-Fermi mixtures in these systems by coupling interlayer excitons to doped charges in a trilayer structure. Their interactions are determined by the interlayer trion, whose spin-selective nature allows excitons to mediate an attractive interaction between charge carriers of only one spin species. Remarkably, we find that this causes the system to become unstable to topological $p + ip$ superconductivity at low temperatures. We then demonstrate a general mechanism to develop and control this unconventional state by tuning the trion binding energy using a solid-state Feshbach resonance.

DOI: 10.1103/PhysRevLett.133.056902

Introduction—Heterostructures of two-dimensional semiconductors are particularly promising platforms to realize exotic phases of matter, such as correlated insulators, Mott-Wigner states, and superconductors [1–15]. Owing to their two-dimensional nature and high effective electron and hole masses, transition metal dichalcogenides (TMDs) in particular can host strongly correlated Bose-Fermi mixtures with fermions realized by doped charges and composite bosons by tightly bound excitons. Doped holes and interlayer excitons interact by forming bound molecular states called trions. The bound-state formation in Bose-Fermi mixtures gives rise to a particularly rich phase diagram, potentially featuring among others coexisting liquids, unconventional superfluids, supersolids, and quantum phase transitions between them [16–27]. In multilayer semiconductor systems scattering between excitons and doped charges can be controlled and strongly enhanced when the energy of the trion is tuned by an external electric field, which is understood as a solid state Feshbach resonance [28,29]. Therefore, two-dimensional materials open new opportunities to realize and study Bose-Fermi mixtures in challenging low-temperature regimes.

A natural route to search for unconventional superconducting states in TMDs [30–37], such as p-wave superconductivity which hosts exotic Majorana edge modes that are pertinent for topological quantum computing [38–40], are thus provided by Bose-Fermi mixtures, as they allow for boson-mediated attractive interactions among charge carriers. However, a controlled realization of p-wave superconductivity remains challenging, as generically s-wave pairing is favored over higher angular momentum states.

Here, we propose a general mechanism to develop and enhance unconventional p-wave superconductivity by tuning Bose-Fermi mixtures of interlayer excitons and holes in a TMD heterostructure. Superconductivity is achieved by hybridizing trions and holes, while the pairing is mediated by excitations of an exciton condensate, as illustrated in Fig. 1. Owing to the spin-selective nature of the trion, only carriers of a single spin species interact attractively, which effectively restricts our model to spinless charge carriers. Then, the Pauli principle forces the Cooper pairs to carry odd angular momentum. Our analysis shows that the superconducting state is topological with $p_x + ip_y$ order. Moreover, the superconducting transition temperature is highly tunable and controllable by an external electric field via a Feshbach resonance.

Experimental setting—We consider a trilayer TMD heterostructure as shown in Fig. 1(a). Interlayer excitons can be optically injected in the bottom two layers at high densities ($\simeq 10^{12}$ cm^{-2}) due to their long lifetime [41,42]. They are strongly bound and essentially act as composite bosons. We assume that excitons are condensed [43,44]. Fermions are introduced in the form of doped holes, which tunnel coherently between the top and middle layer. Hexagonal boron nitride (h-BN) isolates the layers and, to a limited extent, controls the tunneling of charge carriers. Interlayer excitons and charge carriers can bind to a molecular trion state, which allows for controlling the boson-fermion scattering. Tunable effective interactions between holes are then mediated by the exciton condensate; see Fig. 1(b). We specifically consider holes, as it has been found experimentally that the hole tunneling through h-BN is much stronger than electron tunneling [29].

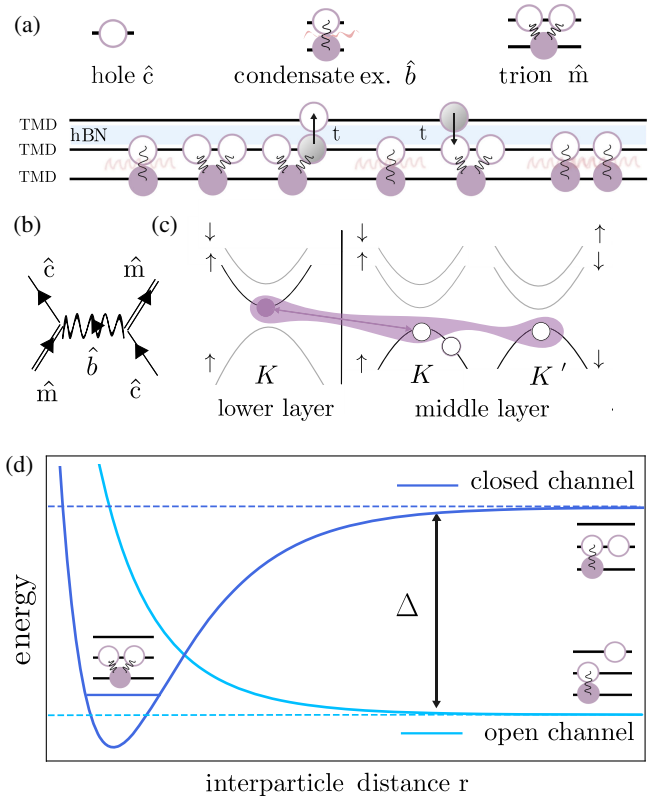

FIG. 1. Tunable Bose-Fermi mixtures. (a) We consider a TMD trilayer heterostructure. The relevant constituents are the charge carriers (holes), that coherently tunnel between the upper and the middle layer with strength t, an interlayer exciton condensate, and the trion bound state. (b) Effective attractive interactions between charge carriers are mediated by the virtual decay of a trion into a hole and a condensate excitation, which then scatters with another hole to create again a trion. (c) The holes in the trion form a singlet. When the exciton condensate is created with a certain spin polarization, for example by circularly polarized light, attractive interactions are only mediated between holes of opposite spin. The exciton (electron hole in say the K valley) forms a trion with a K'-valley hole tunneled from the upper layer. (d) The superconducting state is controlled by a solid-state Feshbach resonance. Effective interactions are enhanced by tuning the threshold of the open channel close to the trion bound state in the closed channel by an external electric field $E_z \propto \Delta$.

We assume that the exciton condensate is optically injected in one valley by circularly polarized light, and thus through spin-momentum locking in one spin state, say the K-valley with spin-↑; see Fig. 1(c). Owing to Pauli blocking, interlayer trion formation is only possible when the holes of the trion, that are both in the same layer, are in a spin singlet, as the triplet is generally unbound [45–47]. For small temperatures compared to the trion bound state energy, two charge carriers that interact with the same exciton to form a trion are thus necessarily in the same spin state. This allows us to consider spinless fermions [43,45–48].

The scattering process between holes and excitons can be controlled by a solid-state Feshbach resonance [28,29], where open and closed channels are tuned relatively to each other by an external electric field E_z; see Fig. 1(d). Strong interactions are obtained when the open channel and the trion bound state are approximately in resonance.

The system of holes $\hat{c}$, trions $\hat{m}$ (also referred to as molecules), and excitons $\hat{x}$ is described by the following effective Hamiltonian (see the Supplemental Material [49] and references therein [50–52]):

$$\hat{H} = \hat{H}_{\text{holes}} + \hat{H}_{\text{trions}} + \hat{H}_{\text{ex}} + g\sum_{\mathbf{k},\mathbf{k}'}\left[\hat{m}^\dagger_{\mathbf{k}}\hat{c}_{\mathbf{k}'}\hat{x}_{\mathbf{k}-\mathbf{k}'} + \text{H.c.}\right], \tag{1}$$

where $\hat{H}_{\text{holes}} = \sum_{\mathbf{k}}(k^2/2m)\hat{c}^\dagger_{\mathbf{k}}\hat{c}_{\mathbf{k}}$ is the kinetic energy of holes of mass m and $\hat{H}_{\text{trions}} = \sum_{\mathbf{k}}[(k^2/2M) + \Delta]\hat{m}^\dagger_{\mathbf{k}}\hat{m}_{\mathbf{k}}$ is the kinetic energy of trions of mass M with $\Delta = edE_z$ being the energy difference of a charge in the upper and the middle layer separated by distance d that is tunable by the electric field E_z. For holes and trions we consider an expansion near the minimum and maximum of the bands, at the K and K' points of the Brillouin zone, where their dispersion is parabolic to a good approximation. The interlayer excitons are governed by $\hat{H}_{\text{ex}} = \sum_{\mathbf{k}}(k^2/2m_x)\hat{x}^\dagger_{\mathbf{k}}\hat{x}_{\mathbf{k}} + (U/2)\sum_{\mathbf{k},\mathbf{p},\mathbf{q}}\hat{x}^\dagger_{\mathbf{k}+\mathbf{q}}\hat{x}^\dagger_{\mathbf{p}-\mathbf{q}}\hat{x}_{\mathbf{k}}\hat{x}_{\mathbf{p}}$, where m_x is the exciton mass and U the strength of the exciton interactions that depends on the dielectric material between the two lowest layers and their distance [41]. Since excitons are injected with low momenta and long-range electron-hole exchange is vanishingly small, due to spatial separation of the electron and the hole, a quadratic dispersion is justified. The last term in the Hamiltonian (1) describes the decay of the molecule into an exciton and a hole of strength g that mediates the effective attractive interactions. Similar Hamiltonians have also been studied in the context of exciton-polariton mediated s-wave superconductivity [53].

We consider the regime in which the binding energy of the exciton is larger than the one of the trion. Then, the exciton's internal structure does not influence the properties of the trion. We are thus allowed to describe the excitons as a Bose gas [54] and assume weak contact interactions. When the excitons condense [55,56], we can expand $\hat{x}_{\mathbf{r}} = \sqrt{n_0} + (1/\sqrt{V})\sum_{\mathbf{k}\neq 0} e^{i\mathbf{k}\mathbf{r}}\hat{x}_{\mathbf{k}}$, where n_0 is the macroscopic condensate density. Performing a Bogoliubov analysis by expanding the purely excitonic part of the Hamiltonian, we obtain

$$\begin{aligned}\hat{H} = \hat{H}_{\text{holes}} + \hat{H}_{\text{trions}} &+ \sum_{\mathbf{k}\neq 0} e_x(k)\hat{b}^\dagger_{\mathbf{k}}\hat{b}_{\mathbf{k}} \\ &+ g\sqrt{n_0}\sum_{\mathbf{k}}\left[\hat{m}^\dagger_{\mathbf{k}}\hat{c}_{\mathbf{k}} + \text{H.c.}\right] \\ &+ g\sum_{\mathbf{k}\neq\mathbf{k}'}\left[\hat{m}^\dagger_{\mathbf{k}}\hat{c}_{\mathbf{k}-\mathbf{k}'}\hat{b}_{\mathbf{k}'} + \text{H.c.}\right],\end{aligned} \tag{2}$$

where $\hat{b}$ are the condensate excitations with energy $e_x(k) = \sqrt{(k^2/2m_x)[(k^2/2m_x) + 2Un_0]}$. The condensate hybridizes the trion and charge bands with strength $g\sqrt{n_0}$. The three-body interaction contains sound excitations of the condensate $\hat{b}$, which are reminiscent of phonon mediated interactions. As the vertex g already includes the tunneling process, the scattering effectively takes place in the same layer. Moreover, as the exciton's Bohr radius is small, a recombination between the constituents can only occur locally when their wave functions have finite overlap. These considerations justify the assumption of contact interactions of strength g [28,57].

The effective trion-exciton-hole coupling g is fixed by the tunnel coupling t of the electrons between the two layers as $g \simeq \sqrt{(2\pi/\mu_{\text{red}}|E_{T,0}|)}t$, where we estimate the bare trion binding energy $E_{T,0} \simeq 6$ meV to be lower than the one reported in Ref. [41] due to the additional h-BN layer between the TMDs, and μ_{red} is the reduced mass of the hole and the exciton; see the Supplemental Material [49]. In our calculations, we assume the tunneling between the two layers to be $t \simeq 0.9$ meV [29]. We typically consider exciton condensate densities of $n_0 \sim 10^{12}$ cm^{-2} and estimate the interactions U between the excitons using a plate capacitor formula as $Un_0 \simeq 10$ meV for $n_0 \sim 10^{12}$ cm^{-2} [41]. For these density regimes, excitons are expected to be tightly bound: similar exciton densities ($\sim 10^{12}$ cm^{-2}) were considered in [58] for even smaller binding energy for the excitons. Moreover, as will be evident later, our results do not depend crucially on a high density of excitons. For the long-range interactions between excitons, decaying as $\sim r^{-3}$, bosons undergo a Berezinskii-Kosterlitz-Thouless transition [59]. To simplify the situation, we consider contact interactions, that, however, capture the linear spectrum at small momenta. The interactions determine the phase fluctuations, and a condensate description of the problem is justified for scales of the sample smaller than the typical coherence length and low temperatures [60,61]. In this parameter regime we expect that our system realizes a good superfluid [62]. Even though detailed numerical studies are lacking for the specific model, we further argue that the condensate fraction is expected to be sizeable as well [63].

Effective attractive interactions—To determine the interactions between doped charges we diagonalize the free fermionic Hamiltonian [17,64]: $\hat{H}_0 = \hat{H}_{\text{holes}} + \hat{H}_{\text{trions}} + g\sqrt{n_0}\sum_{\mathbf{k}}[\hat{m}^\dagger_{\mathbf{k}}\hat{c}_{\mathbf{k}} + \text{H.c.}]$ to obtain the dressed fermions $\hat{f}_{\mathbf{k}} = \alpha_{\mathbf{k}}\hat{m}_{\mathbf{k}} - \beta_{\mathbf{k}}\hat{c}_{\mathbf{k}}$ and $\hat{e}_{\mathbf{k}} = \alpha_{\mathbf{k}}\hat{m}_{\mathbf{k}} + \beta_{\mathbf{k}}\hat{c}_{\mathbf{k}}$, with eigenenergies $\lambda_{e,f}(\mathbf{k}) = (k^2/4)[(M+m)/Mm] + (\Delta/2) \pm \sqrt{\{(k^2/4)[(M-m)/Mm] - (\Delta/2)\}^2 + g^2n_0}$, which define the upper and lower band; see Fig. 2. The gap between the two bands, $\sqrt{\Delta^2 + 4g^2n_0}$, is finite for all values of the electric field and has the minimal value of $2g\sqrt{n_0}$ for $\Delta = 0$. Assuming the Fermi energy to be lower than the energy difference between the two bands and the temperature to be smaller than the gap, we restrict our analysis to the lowest filled band. Then, depending on the sign of the electric field Δ, charges will mainly have trion ($\Delta < 0$) or hole ($\Delta > 0$) character. The resulting Hamiltonian of fermions $\hat{f}$ and condensate excitations $\hat{b}$ is then $\hat{H} = \sum_{\mathbf{k}}[\lambda_f(\mathbf{k}) - \mu]\hat{f}^\dagger_{\mathbf{k}}\hat{f}_{\mathbf{k}} - g\sum_{\mathbf{k}\neq\mathbf{k}'}[\alpha_{\mathbf{k}}\beta_{\mathbf{k}'}\hat{f}^\dagger_{\mathbf{k}}\hat{f}_{\mathbf{k}'}\hat{b}_{\mathbf{k}-\mathbf{k}'} + \text{H.c.}]$.

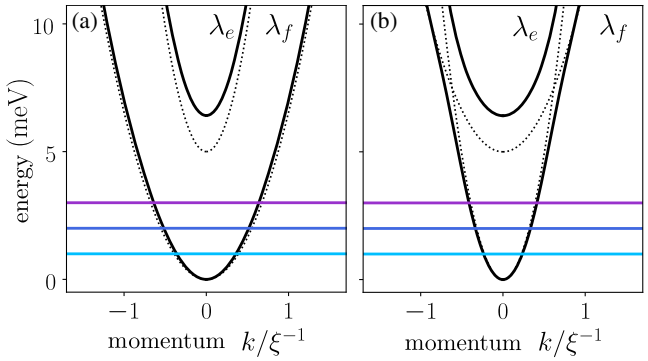

FIG. 2. Hybridized trion and hole bands. Hybridized bands $\lambda_{e/f}(k)$ (solid lines) and bare bands (dotted lines) as a function of momentum k in units of the inverse exciton condensate healing length ξ^{-1}. The Fermi energy (horizontal lines) is chosen to be below the upper band. (a) For $\Delta < 0$, the heavier band is filled, implying that doped charges mainly have trion character. (b) For $\Delta > 0$, the lighter band is filled, and the doped charges will mainly have hole character.

We integrate out the condensate interactions using Wegner flow equations [65], which gives us an effective interaction between charge carries mediated by the excitons. In contrast to a Schrieffer-Wolff transformation this leads to a divergence free potential [23,65–67]; see the Supplemental Material [49]. The resulting effective Hamiltonian is then

$$\hat{H}^{\text{eff}} = \sum_{\mathbf{k}}[\lambda_f(\mathbf{k}) - \mu]\hat{f}^\dagger_{\mathbf{k}}\hat{f}_{\mathbf{k}} + \sum_{\mathbf{k},\mathbf{q}} V_{k,q}\hat{f}^\dagger_{\mathbf{k}-\mathbf{q}}\hat{f}^\dagger_{-\mathbf{k}+\mathbf{q}}\hat{f}_{-\mathbf{k}}\hat{f}_{\mathbf{k}}, \tag{3}$$

with the interactions $V_{k,q} = -(M_{\mathbf{k},\mathbf{q}}M^*_{-\mathbf{k}+\mathbf{q},\mathbf{q}}e_x(\mathbf{q})/\{[\lambda_f(\mathbf{k}) - \lambda_f(\mathbf{k}-\mathbf{q})]^2 + e_x(\mathbf{q})^2\})$ and $M_{k,q} = -g\alpha_{\mathbf{k}}\beta_{\mathbf{k}-\mathbf{q}}$. The effective interaction is thus attractive and directly proportional to the hybridization of molecule and hole bands.

Ginzburg-Landau analysis—To analyze the superconducting order, we identify the pairing instability by looking for unstable solutions in the temporal evolution of the superconducting order parameter [68–70]. In a mean-field formalism, the dynamics of the Cooper pair annihilation operator is

$$\frac{d}{dt}\langle\hat{f}_{\mathbf{k}}\hat{f}_{-\mathbf{k}}\rangle = -\frac{i}{\hbar}\sum_{\mathbf{p}>0}[A_{\mathbf{k},\mathbf{p}} + B_{\mathbf{k},\mathbf{p}}]\langle\hat{f}_{\mathbf{p}}\hat{f}_{-\mathbf{p}}\rangle, \tag{4}$$

with contributions from the noninteracting part of the Hamiltonian $A_{\mathbf{k},\mathbf{p}} = 2(\lambda_f(\mathbf{k}) - \mu)\delta_{\mathbf{k},\mathbf{p}}$ and the two-body interaction $B_{\mathbf{k},\mathbf{p}} = -(2n_{\mathbf{k}} - 1)[V_{\mathbf{k},\mathbf{k}-\mathbf{p}} - V_{\mathbf{k},\mathbf{k}+\mathbf{p}} - V_{-\mathbf{k},-\mathbf{k}-\mathbf{p}} + V_{-\mathbf{k},-\mathbf{k}+\mathbf{p}}]$; $n_{\mathbf{k}} = \langle \hat{f}^{\dagger}_{\mathbf{k}} \hat{f}_{\mathbf{k}} \rangle$ is the thermal expectation value. Here, both A and B are real matrices. The physical interpretation is that if the thermal state is susceptible to form superconductivity, we expect the pairing correlations $\langle \hat{f}_{\mathbf{k}} \hat{f}_{-\mathbf{k}} \rangle$ to grow in time, indicating an unstable solution. To study this instability, we write the time evolution of $\psi_{\mathbf{k}} = \langle \hat{f}_{\mathbf{k}} \hat{f}_{-\mathbf{k}} \rangle$ by means of time-dependent Ginzburg Landau equations [71–73]:

$$\frac{d}{dt}\psi_{\mathbf{k}}(t) = -\frac{\delta \mathcal{F}^{\mathrm{GL}}}{\delta \psi^{*}_{\mathbf{k}}} = -\sum_{\mathbf{p}>0} F^{\mathrm{GL}}_{\mathbf{k},\mathbf{p}} \psi_{\mathbf{p}}. \tag{5}$$

Here $\mathcal{F}^{\mathrm{GL}}$ is the Ginzburg-Landau free energy, which to leading-order reads

$$\mathcal{F}^{\mathrm{GL}} = \sum_{\mathbf{k},\mathbf{p}} \psi^{*}_{\mathbf{k}} F^{\mathrm{GL}}_{\mathbf{k},\mathbf{p}} \psi_{\mathbf{p}} + \mathcal{O}(\psi^4). \tag{6}$$

The associated eigenvectors then determine the structure of the unstable mode. In the Ginzburg-Landau formalism, the eigenvalues of the matrix F^{GL} are proportional to $\propto T - T_c$. Hence, the dominant eigenvalues change their sign when driving the system into the ordered phase. This formalism allows us to identify any possible pairing instability and then to select the most relevant one with the highest critical temperature. By contrast, a mean-field decomposition would require selecting the most relevant pairing channel beforehand. Comparing Eqs. (5) and (4), we obtain the relation $-i\hbar F^{\mathrm{GL}} = C = A + B$; the set of equations can be written in a matrix form as $i\hbar(d/dt)|\psi\rangle = C|\psi\rangle$. The superconducting gap order parameter is related to $\psi_{\mathbf{k}}$ by $\Gamma_{\mathbf{k}} = \sum_{\mathbf{p}} V_{\mathbf{k},\mathbf{p}-\mathbf{k}} \psi_{\mathbf{p}}$. We solve the differential equation by finding the eigenvectors $|\psi\rangle$ and eigenvalues E_{ψ} of $-i\hbar F^{\mathrm{GL}}$. The critical point is then obtained by searching for the temperature at which the imaginary part of some of the E_{ψ} turns positive, indicating the onset of the unstable mode. From the associated eigenvector, we infer the momentum-space structure of the instability. By expanding the order parameter in its angular momentum contribution we find numerically that the p-wave is the only relevant component; see the Supplemental Material [49].

The precise p-wave channel that drives the superconducting instability can be determined separately by minimization of the free energy. To this end, we compare the free energy for the chiral $(p_x + ip_y)$ and nematic (p_x or p_y, respectively) phases. We find that for the instabilities determined as above, the free energy is indeed minimized for the topological $p_x + ip_y$ superconductor; see the Supplemental Material [49], which hosts chiral Majorana edge modes. The Ginzburg-Landau analysis identifies the leading instability, and hence captures the phases near the transition temperature T_c. At even lower temperatures, nonlinearities may stabilize other competing phases.

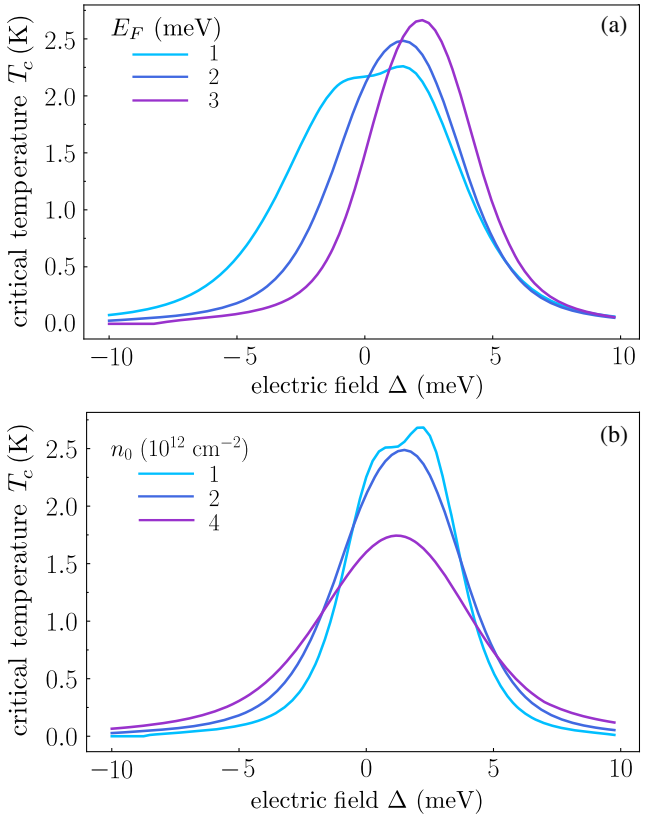

FIG. 3. Critical temperature. We evaluate the critical temperature T_c as a function of the electric field Δ for (a) different Fermi energies at condensate density $n_0 = 2\,10^{12}$ cm^{-2} and for (b) different condensate densities and Fermi energy $E_F = 2$ meV. By tuning the electric field Δ we find that superconductivity can be resonantly enhanced.

Tuning topological superconductivity—We have seen that the attractive interactions sensitively depend on the electric field via the hybridization of molecule and hole bands. This suggests that the superconducting order is controllable by a solid state Feshbach resonance. When adjusting Δ only over a couple of meV, we find that the superconducting transition temperature is tuned by more than 1 order of magnitude; see Fig. 3. The shape of the critical temperature as a function of Δ qualitatively follows the numerically evaluated effective potential in the vicinity of the Fermi surface. By tuning Δ, the hybridization between the two bands can be increased at the relevant energy scales and consequently enhance the critical temperature T_c. The largest T_c is obtained when the hybridization of the bands is largest, which arises approximately when $\Delta \sim 3$ meV. The regime where the superconductivity is suppressed is similarly associated with a decreased hybridization of molecules and holes in proximity of the Fermi surface. When increasing the Fermi energy, we find from our numerical analysis that the maximum of the critical

temperature increases; see Fig. 3(a). This can be understood by the hybridization between the light hole and heavy trion band. When increasing the Fermi energy the band becomes more trionlike for $\Delta \sim |E_T| > 0$. Hence, the hybridized charge carriers $\hat{f}$ attain a larger effective mass when increasing the Fermi energy. This in turn leads to a larger critical temperature.

Varying the condensate density n_0 at a fixed Fermi energy changes both the shape of the hybridized bands $\lambda_{e/f}(\mathbf{k})$ and the condensate healing length $\xi = 1/\sqrt{2m_x U n_0}$. The healing length determines the length scale at which the condensate effectively responds to a perturbation. For larger healing length, we thus expect that the effective attractive interactions are mediated more efficiently; see Fig. 3(b). This is further supported by evaluating the effective attractive interaction for scattering near the Fermi surface which for small fields is given by $V_{k,q} \sim \sqrt{(m_x/U n_0 q^2)}$. The attractive potential near the Fermi surface thus increases when the condensate density decreases, as expected from the scaling of the healing length ξ. While being tunable by the electric field, the critical temperature depends on the thickness of the h-BN, that changes the contact interaction parameter g through the tunneling parameter t. Thus the critical temperature decreases as g is decreased; see the Supplemental Material [49].

Competing effects—In the case of an imperfect but still strongly imbalanced polarization of excitons (say dominant creation of K-valley excitons and small density of K'-valley excitons), an s-wave instability could develop, provided the two exciton species interact. However, owing to the strong imbalance of the Fermi surfaces of the two formed trion species, s-wave superconductivity can only occur at finite momenta and is in general energetically disfavored compared to the normal state. If it was nonetheless allowed to form, it would be strongly suppressed compared to the p-wave channel; see the Supplemental Material [49].

Another competing process is the formation of a Wigner crystal in the hole-doped layer which arises at very low carrier densities [74]. Thus, this regime can be avoided by increasing the charge density.

In cold atom Bose-Fermi mixtures often phase separation arises [26,64]. By contrast in the setup considered here, phase separation is disfavored by long-range Coulomb interactions between the holes, as an increased hole density in phase separated regions leads to a strong increase of the Coulomb interactions.

Discussion and outlook—In this work, we have demonstrated the potential of two-dimensional TMD heterostructures as a tunable platform for realizing correlated Bose-Fermi mixtures of interlayer excitons and doped charges. We have shown that at low temperatures the system stabilizes p-wave topological superconductivity. We propose to utilize solid-state Feshbach resonances to modify the effective interaction strength between the constituents. Experimentally, the superconducting order parameter can be extracted by measuring the ac conductivity. In the superconducting phase the dissipative response of the conductivity then only exhibits spectral weight at frequencies above twice the gap. Within BCS theory, the critical temperature sets the energy scale for the gap, and this places our estimates of these frequencies below ~200 GHz, which are in the experimentally accessible microwave regime. First experimental signatures for the superconducting phase could also be obtained from the single-particle gap, measured optically via the change of the line shape of the top layer exciton [6]. Other possible experimental probes may directly be able to detect the chiral edge states of a p-wave superconductor. Those include spin-polarized scanning tunneling microscopy (STM) [75,76], Josephson STM [77,78], and the Quantum Twisting Microscope [79,80]. These techniques could detect the Majorana zero modes as a signature of topological superconductivity and distinguish between s-wave superconductivity and p-wave superconductivity.

For future studies it will be interesting to explore competing instabilities at low temperatures, such as nematic or density-wave phases, for which nonlinearities and the competition of order parameters need to be taken into account. In this work, we consider the regime of high condensate densities, such that a possible backaction of the charge carriers on the exciton condensate is largely negligible. New exciting phenomena appear in degenerate Bose-Fermi mixtures for low condensate densities, which are interesting to be explored both theoretically and experimentally [25,81,82].

Note added—Milczewski *et al.* explored a complementary scheme for inducing s-wave superconductivity in Bose-Fermi mixtures realized with TMD heterostructures [83].

Acknowledgments—We thank L. Classen, E. Demler, A. Keselman, J. Knolle, and R. Schmidt, for insightful discussions. We acknowledge support from the Deutsche Forschungsgemeinschaft (DFG, German Research Foundation) under Germany's Excellence Strategy–EXC–2111–390814868, DFG Grants No. KN1254/1-2, No. KN1254/2-1, and No. TRR 360–492547816 and from the European Research Council (ERC) under the European Unions Horizon 2020 research and innovation program (Grant Agreement No. 851161), as well as the Munich Quantum Valley, which is supported by the Bavarian state government with funds from the Hightech Agenda Bayern Plus. The work of A. I. was supported by the Swiss National Science Foundation (SNSF) under Grant No. 200021-204076.

Data availability—Data analysis and simulation codes are available on Zenodo upon reasonable request [84].

[1] Y. Cao, V. Fatemi, A. Demir, S. Fang, S. L. Tomarken, J. Y. Luo, J. D. Sanchez-Yamagishi, K. Watanabe, T. Taniguchi, E. Kaxiras, R. C. Ashoori, and P. Jarillo-Herrero, Correlated insulator behaviour at half-filling in magic-angle graphene superlattices, Nature (London) **556**, 80 (2018).

[2] Y. Cao, V. Fatemi, S. Fang, K. Watanabe, T. Taniguchi, E. Kaxiras, and P. Jarillo-Herrero, Unconventional superconductivity in magic-angle graphene superlattices, Nature (London) **556**, 43 (2018).

[3] X. Lu, P. Stepanov, W. Yang, M. Xie, M. A. Aamir, I. Das, C. Urgell, K. Watanabe, T. Taniguchi, G. Zhang, A. Bachtold, A. H. MacDonald, and D. K. Efetov, Superconductors, orbital magnets and correlated states in magic-angle bilayer graphene, Nature (London) **574**, 653 (2019).

[4] A. L. Sharpe, E. J. Fox, A. W. Barnard, J. Finney, K. Watanabe, T. Taniguchi, M. A. Kastner, and D. Goldhaber-Gordon, Emergent ferromagnetism near three-quarters filling in twisted bilayer graphene, Science **365**, 605 (2019).

[5] M. Yankowitz, S. Chen, H. Polshyn, Y. Zhang, K. Watanabe, T. Taniguchi, D. Graf, A. F. Young, and C. R. Dean, Tuning superconductivity in twisted bilayer graphene, Science **363**, 1059 (2019).

[6] Y. Shimazaki, I. Schwartz, K. Watanabe, T. Taniguchi, M. Kroner, and A. Imamoğlu, Strongly correlated electrons and hybrid excitons in a moiré heterostructure, Nature (London) **580**, 472 (2020).

[7] Y. Xu, S. Liu, D. A. Rhodes, K. Watanabe, T. Taniguchi, J. Hone, V. Elser, K. F. Mak, and J. Shan, Correlated insulating states at fractional fillings of moiré superlattices, Nature (London) **587**, 214 (2020).

[8] E. C. Regan, D. Wang, C. Jin, M. I. B. Utama, B. Gao, X. Wei, S. Zhao, W. Zhao, Z. Zhang, K. Yumigeta, M. Blei, J. D. Carlström, K. Watanabe, T. Taniguchi, S. Tongay, M. Crommie, A. Zettl, and F. Wang, Mott and generalized Wigner crystal states in WSe2/WS2 moiré superlattices, Nature (London) **579**, 359 (2020).

[9] L. Wang, E.-M. Shih, A. Ghiotto, L. Xian, D. A. Rhodes, C. Tan, M. Claassen, D. M. Kennes, Y. Bai, B. Kim, K. Watanabe, T. Taniguchi, X. Zhu, J. Hone, A. Rubio, A. N. Pasupathy, and C. R. Dean, Correlated electronic phases in twisted bilayer transition metal dichalcogenides, Nat. Mater. **19**, 861 (2020).

[10] Y. Tang, L. Li, T. Li, Y. Xu, S. Liu, K. Barmak, K. Watanabe, T. Taniguchi, A. H. MacDonald, J. Shan, and K. F. Mak, Simulation of Hubbard model physics in WSe2/WS2 moiré superlattices, Nature (London) **579**, 353 (2020).

[11] Y. Shimazaki, C. Kuhlenkamp, I. Schwartz, T. Smoleński, K. Watanabe, T. Taniguchi, M. Kroner, R. Schmidt, M. Knap, and A. Imamoğlu, Optical signatures of periodic charge distribution in a Mott-like correlated insulator state, Phys. Rev. X **11**, 021027 (2021).

[12] H. Li, S. Li, E. C. Regan, D. Wang, W. Zhao, S. Kahn, K. Yumigeta, M. Blei, T. Taniguchi, K. Watanabe, S. Tongay, A. Zettl, M. F. Crommie, and F. Wang, Imaging two-dimensional generalized Wigner crystals, Nature (London) **597**, 650 (2021).

[13] L. Ma, P. X. Nguyen, Z. Wang, Y. Zeng, K. Watanabe, T. Taniguchi, A. H. MacDonald, K. F. Mak, and J. Shan, Strongly correlated excitonic insulator in atomic double layers, Nature (London) **598**, 585 (2021).

[14] X. Huang, T. Wang, S. Miao, C. Wang, Z. Li, Z. Lian, T. Taniguchi, K. Watanabe, S. Okamoto, D. Xiao, S.-F. Shi, and Y.-T. Cui, Correlated insulating states at fractional fillings of the WS2/WSe2 moiré lattice, Nat. Phys. **17**, 715 (2021).

[15] M. Sun, A. V. Parafilo, K. H. A. Villegas, V. M. Kovalev, and I. G. Savenko, Theory of BCS-like bogolon-mediated superconductivity in transition metal dichalcogenides, New J. Phys. **23**, 023023 (2021).

[16] L. Viverit, C. J. Pethick, and H. Smith, Zero-temperature phase diagram of binary boson-fermion mixtures, Phys. Rev. A **61**, 053605 (2000).

[17] S. Powell, S. Sachdev, and H. P. Büchler, Depletion of the Bose-Einstein condensate in Bose-Fermi mixtures, Phys. Rev. B **72**, 024534 (2005).

[18] H. P. Büchler and G. Blatter, Supersolid versus phase separation in atomic Bose-Fermi mixtures, Phys. Rev. Lett. **91**, 130404 (2003).

[19] T. Enss and W. Zwerger, Superfluidity near phase separation in Bose-Fermi mixtures, Eur. Phys. J. B **68**, 383 (2009).

[20] E. Fratini and P. Pieri, Pairing and condensation in a resonant Bose-Fermi mixture, Phys. Rev. A **81**, 051605 (R) (2010).

[21] D. Ludwig, S. Floerchinger, S. Moroz, and C. Wetterich, Quantum phase transition in Bose-Fermi mixtures, Phys. Rev. A **84**, 033629 (2011).

[22] M. Matuszewski, T. Taylor, and A. V. Kavokin, Exciton supersolidity in hybrid Bose-Fermi systems, Phys. Rev. Lett. **108**, 060401 (2012).

[23] O. Cotleţ, S. Zeytinoğlu, M. Sigrist, E. Demler, and A. Imamoğlu, Superconductivity and other collective phenomena in a hybrid Bose-Fermi mixture formed by a polariton condensate and an electron system in two dimensions, Phys. Rev. B **93**, 054510 (2016).

[24] J. J. Kinnunen, Z. Wu, and G. M. Bruun, Induced p-wave pairing in Bose-Fermi mixtures, Phys. Rev. Lett. **121**, 253402 (2018).

[25] M. Duda, X.-Y. Chen, A. Schindewolf, R. Bause, J. von Milczewski, R. Schmidt, I. Bloch, and X.-Y. Luo, Transition from a polaronic condensate to a degenerate Fermi gas of heteronuclear molecules, Nat. Phys. **19**, 720 (2023).

[26] K. Suzuki, T. Miyakawa, and T. Suzuki, p-wave superfluid and phase separation in atomic Bose-Fermi mixtures, Phys. Rev. A **77**, 043629 (2008).

[27] R. M. Kalas, A. V. Balatsky, and D. Mozyrsky, Odd-frequency pairing in a binary mixture of bosonic and fermionic cold atoms, Phys. Rev. B **78**, 184513 (2008).

[28] C. Kuhlenkamp, M. Knap, M. Wagner, R. Schmidt, and A. Imamoğlu, Tunable Feshbach resonances and their spectral signatures in bilayer semiconductors, Phys. Rev. Lett. **129**, 037401 (2022).

[29] I. Schwartz, Y. Shimazaki, C. Kuhlenkamp, K. Watanabe, T. Taniguchi, M. Kroner, and A. Imamoğlu, Electrically tunable Feshbach resonances in twisted bilayer semiconductors, Science **374**, 336 (2021).

[30] Y.-T. Hsu, A. Vaezi, M. H. Fischer, and E.-A. Kim, Topological superconductivity in monolayer transition metal dichalcogenides, Nat. Commun. **8**, 14985 (2017).

[31] G. Margalit, E. Berg, and Y. Oreg, Theory of multi-orbital topological superconductivity in transition metal dichalcogenides, Ann. Phys. (Amsterdam) **435**, 168561 (2021).
[32] C. Lane and J.-X. Zhu, Identifying topological superconductivity in two-dimensional transition-metal dichalcogenides, Phys. Rev. Mater. **6**, 094001 (2022).
[33] M. M. Scherer, D. M. Kennes, and L. Classen, Chiral superconductivity with enhanced quantized Hall responses in moiré transition metal dichalcogenides, npj Quantum Mater. **7**, 100 (2022).
[34] A. Julku, J. J. Kinnunen, A. Camacho-Guardian, and G. M. Bruun, Light-induced topological superconductivity in transition metal dichalcogenide monolayers, Phys. Rev. B **106**, 134510 (2022).
[35] V. Crépel, D. Guerci, J. Cano, J. H. Pixley, and A. Millis, Topological superconductivity in doped magnetic moiré semiconductors, Phys. Rev. Lett. **131**, 056001 (2023).
[36] Y. W. Li *et al.*, Observation of topological superconductivity in a stoichiometric transition metal dichalcogenide 2M-WS2, Nat. Commun. **12**, 2874 (2021).
[37] A. K. Nayak, A. Steinbok, Y. Roet, J. Koo, G. Margalit, I. Feldman, A. Almoalem, A. Kanigel, G. A. Fiete, B. Yan, Y. Oreg, N. Avraham, and H. Beidenkopf, Evidence of topological boundary modes with topological nodal-point superconductivity, Nat. Phys. **17**, 1413 (2021).
[38] X.-L. Qi and S.-C. Zhang, Topological insulators and superconductors, Rev. Mod. Phys. **83**, 1057 (2011).
[39] J. Alicea, New directions in the pursuit of Majorana fermions in solid state systems, Rep. Prog. Phys. **75**, 076501 (2012).
[40] C. Kallin and J. Berlinsky, Chiral superconductors, Rep. Prog. Phys. **79**, 054502 (2016).
[41] L. A. Jauregui, A. Y. Joe, K. Pistunova, D. S. Wild, A. A. High, Y. Zhou, G. Scuri, K. De Greve, A. Sushko, C.-H. Yu, T. Taniguchi, K. Watanabe, D. J. Needleman, M. D. Lukin, H. Park, and P. Kim, Electrical control of interlayer exciton dynamics in atomically thin heterostructures, Science **366**, 870 (2019).
[42] N. P. Wilson, W. Yao, J. Shan, and X. Xu, Excitons and emergent quantum phenomena in stacked 2D semiconductors, Nature (London) **599**, 383 (2021).
[43] Z. Wang, D. A. Rhodes, K. Watanabe, T. Taniguchi, J. C. Hone, J. Shan, and K. F. Mak, Evidence of high-temperature exciton condensation in two-dimensional atomic double layers, Nature (London) **574**, 76 (2019).
[44] M. Troue, J. Figueiredo, L. Sigl, C. Paspalides, M. Katzer, T. Taniguchi, K. Watanabe, M. Selig, A. Knorr, U. Wurstbauer, and A. W. Holleitner, Extended spatial coherence of interlayer excitons in $MoSe_2/WSe_2$ heterobilayers, Phys. Rev. Lett. **131**, 036902 (2023).
[45] O. Witham, R. J. Hunt, and N. D. Drummond, Stability of trions in coupled quantum wells modeled by two-dimensional bilayers, Phys. Rev. B **97**, 075424 (2018).
[46] R. Tempelaar and T. C. Berkelbach, Many-body simulation of two-dimensional electronic spectroscopy of excitons and trions in monolayer transition metal dichalcogenides, Nat. Commun. **10**, 3419 (2019).
[47] D. D. Dai and L. Fu, Strong-coupling phases of trions and excitons in electron-hole bilayers at commensurate densities, Phys. Rev. Lett. **132**, 196202 (2024).
[48] P. Rivera, J. R. Schaibley, A. M. Jones, J. S. Ross, S. Wu, G. Aivazian, P. Klement, K. Seyler, G. Clark, N. J. Ghimire, J. Yan, D. G. Mandrus, W. Yao, and X. Xu, Observation of long-lived interlayer excitons in monolayer MoSe2–WSe2 heterostructures, Nat. Commun. **6**, 1 (2015).
[49] See Supplemental Materials at http://link.aps.org/supplemental/10.1103/PhysRevLett.133.056902 for details on the calculations reported in the main text, as well as discussions on less stringent experimental scenarios. First, we derive the model Hamiltonian and coupling parameters from the microscopic model. Next, we analyze the imperfect exciton polarization scenario. Following this, we elaborate on the method used to trace out the bosonic degrees of freedom. In the final sections, we examine the symmetry of the order parameter, argue that the system exhibits instability towards topological $p + ip$ superconductivity, and comment on the dependence of the critical temperature on the thickness of the hBN layer.
[50] E. Barré, O. Karni, E. Liu, A. L. O'Beirne, X. Chen, H. B. Ribeiro, L. Yu, B. Kim, K. Watanabe, T. Taniguchi, K. Barmak, C. H. Lui, S. Refaely-Abramson, F. H. da Jornada, and T. F. Heinz, Optical absorption of interlayer excitons in transition-metal dichalcogenide heterostructures, Science **376**, 406 (2022).
[51] E. Wietek, M. Florian, J. Göser, T. Taniguchi, K. Watanabe, A. Högele, M. M. Glazov, A. Steinhoff, and A. Chernikov, Nonlinear and negative effective diffusivity of interlayer excitons in moiré-free heterobilayers, Phys. Rev. Lett. **132**, 016202 (2024).
[52] F. Chevy and C. Mora, Ultra-cold polarized Fermi gases, Rep. Prog. Phys. **73**, 112401 (2010).
[53] F. P. Laussy, A. V. Kavokin, and I. A. Shelykh, Exciton-polariton mediated superconductivity, Phys. Rev. Lett. **104**, 106402 (2010).
[54] I. Amelio, N. D. Drummond, E. Demler, R. Schmidt, and A. Imamoglu, Polaron spectroscopy of a bilayer excitonic insulator, Phys. Rev. B **107**, 155303 (2023).
[55] M. M. Fogler, L. V. Butov, and K. S. Novoselov, High-temperature superfluidity with indirect excitons in van der Waals heterostructures, Nat. Commun. **5**, 1 (2014).
[56] S. Gupta, A. Kutana, and B. I. Yakobson, Heterobilayers of 2D materials as a platform for excitonic superfluidity, Nat. Commun. **11**, 2989 (2020).
[57] C. Fey, P. Schmelcher, A. Imamoglu, and R. Schmidt, Theory of exciton-electron scattering in atomically thin semiconductors, Phys. Rev. B **101**, 195417 (2020).
[58] R. Qi, Q. Li, Z. Zhang, S. Chen, J. Xie, Y. Ou, Z. Cui, D. D. Dai, A. Y. Joe, T. Taniguchi, K. Watanabe, S. Tongay, A. Zettl, L. Fu, and F. Wang, Electrically controlled interlayer trion fluid in electron-hole bilayers, arXiv:2312.03251.
[59] A. Filinov, N. V. Prokof'ev, and M. Bonitz, Berezinskii-Kosterlitz-Thouless transition in two-dimensional dipole systems, Phys. Rev. Lett. **105**, 070401 (2010).
[60] D. S. Petrov, D. M. Gangardt, and G. V. Shlyapnikov, Low-dimensional trapped gases, J. Phys. IV France. **116**, 5 (2004).
[61] A. Boudjemâa and G. V. Shlyapnikov, Two-dimensional dipolar Bose gas with the roton-maxon excitation spectrum, Phys. Rev. A **87**, 025601 (2013).

[62] A. Filinov, N. V. Prokof'ev, and M. Bonitz, Berezinskii-Kosterlitz-Thouless transition in two-dimensional dipole systems, Phys. Rev. Lett. **105**, 070401 (2010).
[63] E. Arrigoni, M. Knap, and W. von der Linden, Extended self-energy functional approach for strongly correlated lattice bosons in the superfluid phase, Phys. Rev. B **84**, 014535 (2011).
[64] F. M. Marchetti, C. J. M. Mathy, D. A. Huse, and M. M. Parish, Phase separation and collapse in Bose-Fermi mixtures with a Feshbach resonance, Phys. Rev. B **78**, 134517 (2008).
[65] F. J. Wegner, Flow equations for Hamiltonians, Nucl. Phys. B, Proc. Suppl. **90**, 141 (2000).
[66] S. D. Glazek and K. G. Wilson, Perturbative renormalization group for Hamiltonians, Phys. Rev. D **49**, 4214 (1994).
[67] A. Mielke, Calculating critical temperatures of superconductivity from a renormalized Hamiltonian, Europhys. Lett. **40**, 195 (1997).
[68] A. Abrikosov, L. Gor'kov, and I. Dzyaloshinski, *Methods of Quantum Field Theory in Statistical Physics*, Dover Books on Physics Series (Dover Publications, New York, 1975).
[69] D. Pekker, M. Babadi, R. Sensarma, N. Zinner, L. Pollet, M. W. Zwierlein, and E. Demler, Competition between pairing and ferromagnetic instabilities in ultracold Fermi gases near Feshbach resonances, Phys. Rev. Lett. **106**, 050402 (2011).
[70] M. Knap, M. Babadi, G. Refael, I. Martin, and E. Demler, Dynamical Cooper pairing in nonequilibrium electron-phonon systems, Phys. Rev. B **94**, 214504 (2016).
[71] M. J. Stephen and H. Suhl, Weak time dependence in pure superconductors, Phys. Rev. Lett. **13**, 797 (1964).
[72] P. W. Anderson, N. R. Werthamer, and J. M. Luttinger, An additional equation in the phenomenology of superconductivity: Resistive effects, Phys. Rev. **138**, A1157 (1965).
[73] E. Abrahams and T. Tsuneto, Time variation of the Ginzburg-Landau order parameter, Phys. Rev. **152**, 416 (1966).
[74] T. Smoleński, P. E. Dolgirev, C. Kuhlenkamp, A. Popert, Y. Shimazaki, P. Back, X. Lu, M. Kroner, K. Watanabe, T. Taniguchi, I. Esterlis, E. Demler, and A. Imamoğlu, Signatures of Wigner crystal of electrons in a monolayer semiconductor, Nature (London) **595**, 53 (2021).
[75] B. Jäck, Y. Xie, and A. Yazdani, Detecting and distinguishing Majorana zero modes with the scanning tunnelling microscope, Nat. Rev. Phys. **3**, 541 (2021).
[76] J. Feldmeier, W. Natori, M. Knap, and J. Knolle, Local probes for charge-neutral edge states in two-dimensional quantum magnets, Phys. Rev. B **102**, 134423 (2020).
[77] B. Jäck, M. Eltschka, M. Assig, M. Etzkorn, C. R. Ast, and K. Kern, Critical Josephson current in the dynamical Coulomb blockade regime, Phys. Rev. B **93**, 020504(R) (2016).
[78] M. T. Randeria, B. E. Feldman, I. K. Drozdov, and A. Yazdani, Scanning Josephson spectroscopy on the atomic scale, Phys. Rev. B **93**, 161115(R) (2016).
[79] F. Pichler, W. Kadow, C. Kuhlenkamp, and M. Knap, Probing magnetism in moiré heterostructures with quantum twisting microscopes, arXiv:2402.04311.
[80] A. Inbar, J. Birkbeck, J. Xiao, T. Taniguchi, K. Watanabe, B. Yan, Y. Oreg, A. Stern, E. Berg, and S. Ilani, The quantum twisting microscope, Nature (London) **614**, 682 (2023).
[81] L. D. Marco, G. Valtolina, K. Matsuda, W. G. Tobias, J. P. Covey, and J. Ye, A degenerate Fermi gas of polar molecules, Science **363**, 853 (2019).
[82] Z. Z. Yan, Y. Ni, A. Chuang, P. E. Dolgirev, K. Seetharam, E. Demler, C. Robens, and M. Zwierlein, Dissipationless flow in a Bose-Fermi mixture, arXiv:2304.07663.
[83] J. von Milczewski, X. Chen, A. Imamoğlu, and R. Schmidt, Superconductivity induced by strong electron-exciton coupling in doped atomically thin semiconductor heterostructures, arXiv:2310.10726.
[84] C. Zerba, C. Kuhlenkamp, A. Imamoglu, and M. Knap, Realizing Topological Superconductivity in Tunable Bose-Fermi Mixtures with Transition Metal Dichalcogenide Heterostructures, Zenodo (2023), 10.5281/zenodo.10008122.